Journal of the Korean Magnetic Resonance Society **2013**, *17,* 24-29
DOI 10.6564/JKMRS.2013.17.1.024

Structural Characteristics of 3- and 4-Coordinate Borons from ^{11}B MAS NMR and Single-Crystal NMR in the Nonlinear Optical Material BiB_3O_6

Woo Young Kim[1] and Ae Ran Lim[1,2,*]

[1]Department of Carbon Fusion Engineering, Jeonju University, Jeonju 560-759, Korea
[2] Department of Science Education, Jeonju University, Jeonju 560-759, Korea

Received April 5, 2013; Revised June 04, 2013; Accepted June 10, 2013

Abstract The structural characteristics of 4-coordinate BO_4 [B(1)] and 3-coordinate BO_3 [B(2)] groups in BiB_3O_6 were studied by ^{11}B magic angle spinning (MAS) and single-crystal nuclear magnetic resonance (NMR) spectroscopy. The spin–lattice relaxation time in the laboratory frame, T_1, for ^{11}B decreased slowly with increasing temperature, whereas the spin–lattice relaxation times in the rotating frame, $T_{1\rho}$, for B(1) and B(2), which differed from T_1, were nearly constant. Further, $T_{1\rho}$ for B(1) and B(2) showed very similar trends, although the $T_{1\rho}$ value of B(2) was shorter than that of B(1). The 3-coordinate BO_3 and 4-coordinate BO_4 were distinguished by ^{11}B MAS NMR spectrum and $T_{1\rho}$.

Keywords BiB_3O_6, Boron, Nonlinear optical material, MAS NMR, Spin–lattice relaxation time

Introduction

BiB_3O_6 was first described in early 1962 by investigation of the binary phase diagram for Bi_2O_3–B_2O_3 [1]. Later, in 1982, the first single crystals of BiB_3O_6 were grown[2-4]. BiB_3O_6 single crystals have been of considerable interest during the last decade owing to their highly efficient nonlinear optical (NLO) properties in second-harmonic generation[5] as well as third-harmonic generation applications[6]. The complex structural characteristics of borate compounds lead to a great variety in the selection of structural types favorable for NLO effects, and the anionic group theory can be used to systematically elucidate which structural unit is most likely to exhibit large nonlinearities. In particular, many studies discussed the bond parameter methods, anharmonic oscillator models, and bond charge model[7, 8]. Chen's group[9] has turned its attention to borates. They recognized that borate compounds have numerous structural types because borate atoms may have either 3- or 4-fold coordination. In addition, they[10-12] suggested that the π-conjugated orbital system of an acentric planar organic molecule with charge transfer between donor and acceptor substituent groups was mainly responsible for the presence of a large second-order susceptibility in such molecules. Previous investigations have established that bismuth triborate, BiB_3O_6, has superior NLO properties as compared to other borate crystals1[13-17]; for example, its effective nonlinear coefficient is 4 times that of LiB_3O_5 and 1.5 times that of BaB_2O_4[18]. BiB_3O_6 is a non-ferroelectric, polar crystal with outstanding physical properties, and it has quickly come to be recognized as an excellent NLO material [19-24].

The relaxation mechanisms of BiB_3O_6 have been studied by examining the ^{11}B spin–lattice relaxation time, T_1, in the laboratory frame[25]. However, the relaxation times of the 4-coordinate B(1) atoms and

* Address correspondence to: **Ae Ran Lim,** Department of Science Education, Jeonju University, Jeonju 560-759, Korea, Tel: +82-(0)63-220-2514; Fax: +82-(0)63-220-2053; E-mail: aeranlim@hanmail.net

3-coordinate B(2) atoms cannot be distinguished because the central resonance lines of B(1) and B(2) overlap. To obtain detailed information about the environments of the two types of borons, it is necessary to measure the spin–lattice relaxation times in the rotating frame $T_{1\rho}$ of ^{11}B nuclei.

In this paper, the structural characteristics of 3-coordinate BO_3 and 4-coordinate BO_4 groups in BiB_3O_6 were studied using ^{11}B magic angle spinning (MAS) nuclear magnetic resonance (NMR) and single-crystal NMR spectroscopy. These results can be used to develop guidelines for identifying and developing NLO materials.

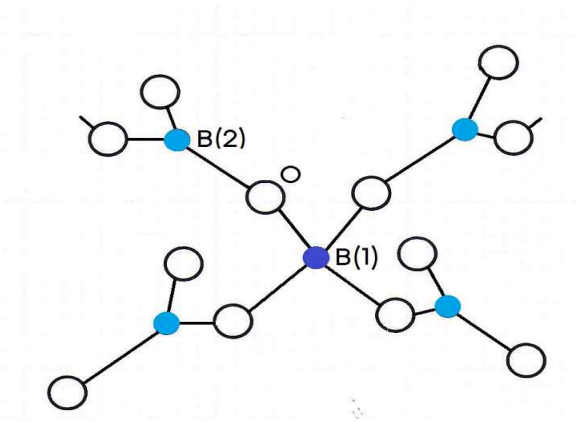

Figure 1. View of BO_4 tetrahedra, B(1), and BO_3 triangles, B(2), in BiB_3O_6.

Crystal structure

BiB_3O_6 crystals have a monoclinic structure with space group C2 (C_2^3) and cell parameters a=7.116 Å, b=4.993 Å, c=6.508 Å, and β=105.62° [26]. These crystals consist of $(B_3O_6)^{3-}$ rings forming sheets of corner-sharing BO_3 triangles and BO_4 tetrahedra, linked by 6-coordinate bismuth cations[27], as shown in Fig. 1. A lone-pair electron is located on the bismuth cation. The structure contains sheets formed by BO_3 triangles and BO_4 tetrahedra in a 2:1 ratio. Here, each BO_4 tetrahedron is connected to four BO_3 triangles, each of which serves as a link to a further BO_4 tetrahedron. The bond lengths of the B(2)–O triangle (1.373 Å) are much shorter than those of the B(1)–O tetrahedron (1.465 Å) (4).

Experimental methods

Single crystals of BiB_3O_6 were grown by the top-seeded method. The as-grown BiB_3O_6 crystals were transparent and colorless, and 3 mm × 3 mm × 2 mm in size.

The NMR signals of the ^{11}B nuclei in the BiB_3O_6 single crystals were measured using a Bruker DSX 400 FT NMR spectrometer at the Korea Basic Science Institute. The static magnetic field was 9.4 T, and the central radio frequency was set at $\omega_o/2\pi$ =

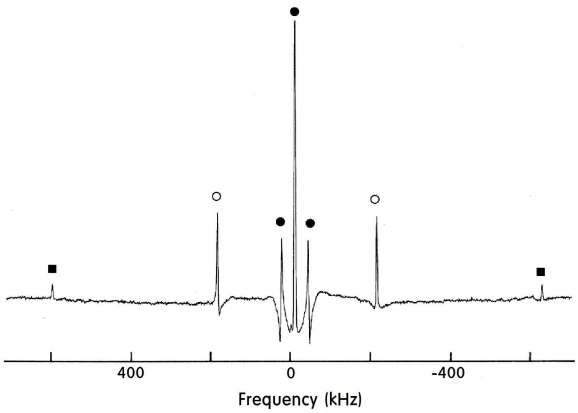

Figure 2. ^{11}B NMR spectrum of BiB_3O_6 single crystal at room temperature [■: B(1), ○ and ●: B(2)].

128.34 MHz for the ^{11}B nucleus. The spin–lattice relaxation times in the laboratory frame, T_1, were measured by applying a pulse sequence of $\pi/2$–t–$\pi/2$. The width of the $\pi/2$ pulse was 0.25 μs for ^{11}B. The nuclear magnetizations $S(t)$ of the ^{11}B nuclei at time t after the $\pi/2$ pulse were determined from each saturation recovery sequence following the pulse.

In addition, to obtain the spin–lattice relaxation time in the rotating frame, $T_{1\rho}$, solid-state NMR experiments were performed using a Bruker 400 MHz NMR spectrometer. An MAS ^{11}B NMR experiment was performed at a Larmor frequency of 128.34 MHz. The samples were placed in the 4 mm cross-polarization/MAS probe as powders. The MAS

rate was set to 13 kHz for ^{11}B MAS to minimize the spinning sideband overlap. The width of the $\pi/2$ pulse for ^{11}B was 2.5 μs, which corresponds to a spin-locking field strength of 100 kHz.

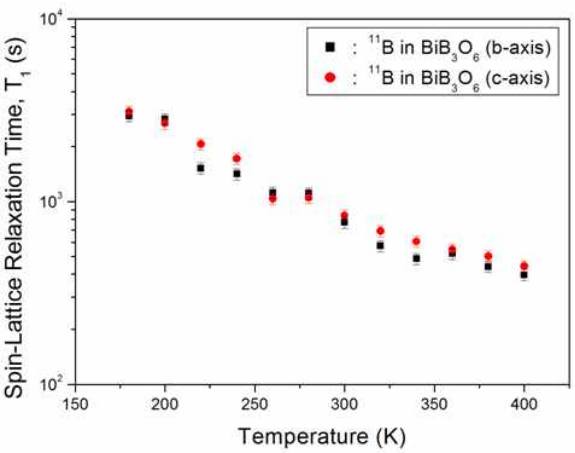

Figure 3. Temperature dependences of the spin–lattice relaxation time in the laboratory frame T_1 for ^{11}B nucleus in BiB_3O_6 single crystal.

Experimental results and discussion

The ^{11}B (I = 3/2) NMR spectrum of BiB_3O_6 crystals usually consists of a central line and two satellite lines. Here, when the magnetic field was applied along the b- axes of the crystal, three groups of resonance lines were observed. The ^{11}B spectrum obtained at room temperature indicates the presence of two types of chemically inequivalent ^{11}B nuclei, denoted B(1) and B(2), as shown in Fig. 2. The difference in intensity ratios in the spectrum is associated with chemically inequivalent positions of ^{11}B atoms in the unit cell[19]. The weaker and stronger signals represent the ^{11}B NMR lines for B(1) and B(2), respectively. Further, the two signals for the B(2) nucleus represent magnetically inequivalent but chemically equivalent positions[25]. In the BiB_3O_6 spectra, the zero point of the horizontal axis corresponds to the resonance frequency of the ^{11}B nucleus (i.e., 128.34 MHz). The central transition is virtually unshifted by the quadrupole interaction, and the separations between the lines for both B(1) and B(2) do not vary with temperature. Thus, we can conclude that the quadrupole parameters of B(1) and B(2) differ and are independent of temperature. The no variation in the splitting of the ^{11}B resonance lines with temperature indicates that the electric field gradient tensor (EFG) at the B sites remains unchanged, which in turn means that the atoms neighboring the ^{11}B nuclei are not displaced when the temperature is varied.

The ^{11}B spin–lattice relaxation times in the laboratory frame, T_1, for B(1) and B(2) cannot be distinguished because the central lines of B(1) and B(2) overlap. Thus, the relaxation times of the 4-coordinate B(1) and 3-coordinate B(2) cannot be distinguished. Therefore, T_1 was measured by applying the saturation recovery method to the central resonance line. The magnetizations of the ^{11}B nuclei were measured at several temperatures. The recovery traces for the central resonance line of ^{11}B with dominant quadrupole relaxation can be expressed as combinations of two exponential functions. T_1 was determined directly from the slope of a plot of log $[S(\infty) - S(t)]/S(\infty)$ versus time t. The recovery traces at each temperature are different, and the slopes of the traces decrease with increasing temperature. The temperature dependences of T_1 for ^{11}B NMR determined with the magnetic field along the b- and

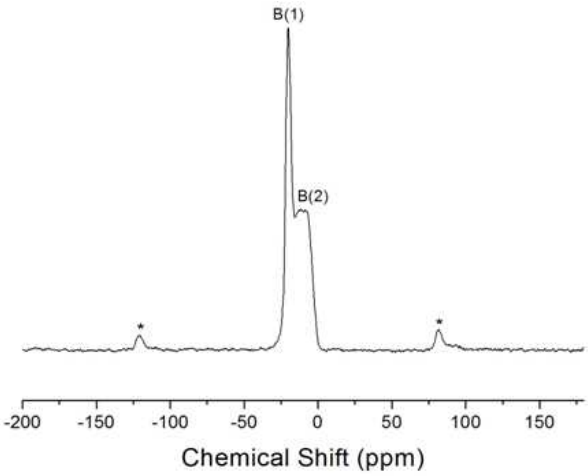

Figure 4. ^{11}B MAS NMR spectrum of BiB_3O_6 at room temperature [B(1): 4-coordinate BO_4, B(2): 3-coordinate BO_3].

c-axes are shown in Fig. 3. The T_1 values for both

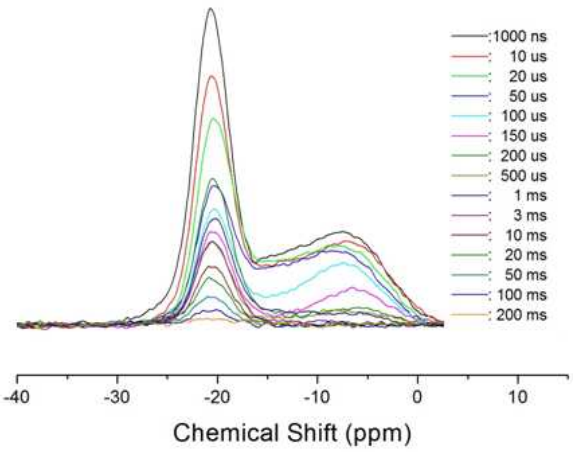

Figure 5. Saturation recovery of B(1) and B(2) in BiB_3O_6 as a function of delay time *t* at room temperature.

crystal directions are the same within the experimental error range. The relaxation time decreased with increasing temperature, and the T_1 values for ^{11}B were very long (400–3000 *s*).

The structure of the boron in BiB_3O_6 was analyzed by a solid-state NMR method. The ^{11}B MAS NMR spectrum of BiB_3O_6 at room temperature is shown in Fig. 4. It consists of two peaks at chemical shifts of δ = –20.13 and –10.24 ppm, which indicate the two types of boron. The spinning sidebands are marked with asterisks. The signals at chemical shifts of –20.13 ppm and –10.24 ppm are assigned to the tetrahedral BO_4 [B(1)] and trigonal BO_3 [B(2)] groups, respectively. The former signal is strong, whereas the latter is weak and broad. The 4-coordinate B(1) and 3-coordinate B(2) is consistent with a ratio of 1:2 in a unit cell.

Further, the ^{11}B spin-lattice relaxation times in the rotating frame, $T_{1\rho}$, were taken at several temperatures in BiB_3O_6. The nuclear magnetization recovery traces obtained for B(1) and B(2) were described by a single exponential function, $S(t) = S(\infty)\exp(-t/T_{1\rho})$ [28]: the recovery traces showed a single exponential decay at all temperatures. The recovery traces of the ^{11}B MAS NMR spectrum are shown in Fig. 5 as a function of delay time from 1000 *ns* to 200 *ms*. The slopes of the recovery traces are nearly the same at each temperature. The temperature dependences of the ^{11}B spin–lattice relaxation time in the rotating frame, $T_{1\rho}$, for B(1) and B(2) are shown in Fig. 6. $T_{1\rho}$ is nearly temperature independent, and the values for 4-coordinate B(1) and 3-coordinate B(2) show similar trends, with that of B(1) being slightly longer than that of B(2). The relaxation time for ^{11}B is very short (0.2–0.1 *ms*).

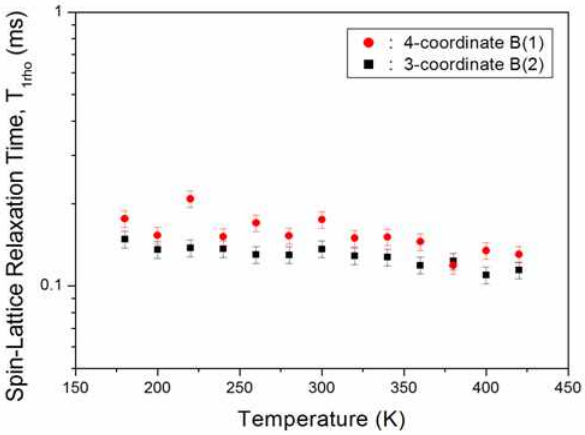

Figure 6. Temperature dependences of the spin–lattice relaxation time in the rotating frame $T_{1\rho}$ for B(1) and B(2) in BiB_3O_6.

Conclusion

The spin–lattice relaxation time in the rotating frame $T_{1\rho}$ is generally similar to the spin–lattice relaxation time in the laboratory frame T_1. Measurements of $T_{1\rho}$ have the advantage of probing molecular motion in the kilohertz range, whereas T_1 reflects motion in the megahertz range. ^{11}B MAS and ^{11}B single-crystal NMR spectroscopy are well-established analytical tools used in several areas to examine the diverse structural chemistry of boron. Here we used them to examine the structural characteristics of 4-coordinate BO_4 [B(1)] and 3-coordinate BO_3 [B(2)] groups in BiB_3O_6. The T_1 values for ^{11}B decreased slowly with increasing temperature, whereas $T_{1\rho}$ was nearly constant. T_1 differed greatly from $T_{1\rho}$; $T_1 \sim 800$ *s* and $T_{1\rho} \sim 0.15$ *ms* at room temperature. Further, $T_{1\rho}$ for

4-coordinate B(1) and 3-coordinate B(2) showed very similar trends. The results made it possible to distinguish 3-coordinate BO_3 and 4-coordinate BO_4 boron using ^{11}B MAS NMR spectrum and $T_{1\rho}$. This research can be used to explain the structure–property relationships in most known NLO crystals of various structural types and to establish guidelines for identifying and developing new NLO materials.

Acknowledgement

This research was supported by the Basic Science Research program through the National Research Foundation of Korea (NRF) funded by the Ministry of Education, Science, and Technology (2012001763).

References

1. E. M. Levin, C. L. McDaniel, *J. Am. Ceram. Soc.* **45**, 355 (1962).
2. J. Liebertz, *Z. Kristallogr.* **158**, 319 (1982).
3. J. Liebertz, *Progr. Crystal Growth Charact*. **6**, 361 (1983).
4. R. Frohlich, L. Bohaty, J. Liebertz, *Acta Crystallogr*. C **40**, 343 (1984).
5. H. Lingxiong, L. Xiang, Z. Ge, H. Chenghui, W. Yong, *J. Phys. D: Appl. Phys*. **42**, 225109 (2009).
6. A. Majchrowski, J. Ebothe, K. Ozga, I.V. Kityk, A.H. Reshak, T. Lukasiewicz, M.G. Brik, *J. Phys. D: Appl. Phys*. **43**, 15103 (2010).
7. M. Ghotibi, M. Ebrahim-Zadeh, A. Majchrowski, E. Michalski, I.V. Kityk, *Opt. Lett*. **29**, 2530 (2004).
8. M. Ghotbi, Z. Sun, A. Majchrowski, E. Michalski, I.V. Kityk, *Appl. Phys. Lett*. **89**, 173124 (2006).
9. C. T. Chen, *Development of New Nonlinear Optical Crystals in the Borate Series*, Harwood Academic Publishers, Switzerland, 1993.
10. C. T. Chen, B. C. Wu, A. Jiang, G. M. You, *Sci. Sinica B* **18**, 235 (1985).
11. Y. C. Wu, C. T. Chen, *Acta Phys. Sinica* **35**, 1 (1986).
12. C. T. Chen, Y. C. Wu, A. Jiang, B. C. Wu, G. M. You, R. K. Li, S. J. Lin, *J. Opt. Soc. Am. B* **6**, 616 (1989).
13. D. Xue, K. Betzler, D. Hesse, D. Lammers, *Phys. Stat. Solidi A* **176**, R1 (1999).
14. Z. Lin, Z. Wang, C. T. Chen, M. H. Lee, *J. Appl. Phys.* **90**, 5585 (2001).
15. B. Teng, J. Wang, Z. Wang, H. Jiang, X. Hu, R. Song, H. Liu, Y. Liu, J. Wei, Z. Shao, *J. Cryst. Growth* **224**, 280 (2001).
16. Z. Wang, B. Teng, K. Fu, X. Xu, R. Song, C. Du, H. Jiang, J. Wang, Y. Liu, Z. Shao, *Opt. Commun*. **202**, 217 (2002).
17. C. Czeranowsky, E. Heumann, G. Huber, *Opt. Lett*. **28**, 432 (2003).
18. Ya. V. Burak, I. V. Kityk, T. Berko, Ya. O. Dovgii, *Ukr. Phys. Journal* V. **32**, 312 (1992).
19. H. Hellwig, J. Liebertz, L. Bohaty, *Solid State Commun*. **109**, 249 (1999).
20. H. Hellwig, J. Liebertz, L. Bohaty, *J. Appl. Phys*. **88**, 240 (2000).
21. C. Du, Z. Wang, J. Liu, X. Xu, B. Teng, K. Fu, J. Wang, Y. Liu, Z. Shao, *Appl. Phys*. B **73**, 215 (2001).
22. I. V. Kityk, A. Majchrowski, *Opt. Mater.* **25**, 33 (2004).
23. A. A. Kaminskii, P. Becker, L. Bohaty, K. Ueda, K. Takaichi, J. Hanuza, M. Maczka, H. J. Eichler, G. M. A. Gad, *Opt. Commun*. **206**, 179 (2002).
24. J.H. Jang, I.H. Yoon, C.S. Yoon, *Opt. Mater*. **31**, 781 (2009).

25. A. R. Lim, J.H. Jang, I. H. Yoon, C.S. Yoon, *Phys. Stat. Solidi* B **247**, 2290 (2010).
26. P. Becker, J. Liebertz, L. Bohaty, *J. Cryst. Growth*. **203**, 149 (1999).
27. R. Frohlich, L. Bohaty, J. Liebertz, *Acta. Crystallogr. C: Cryst. Struct. Commun*. **40**, 343 (1984).
28. J. L. Koenig, *Spectroscopy of Polymer*, Elsevier, New York, (1999).